




Article

Three-Dimensional Bone Alignment from Cone-Beam Computed-Tomography Scans in Weight-Bearing and Clinical Outcomes Following the Modified Grice–Green Surgical Procedure for Adult Acquired Flatfoot

Giulio Sacchetti ¹, Claudio Belvedere ^{1,*} , Maurizio Ortolani ¹ , Alberto Leardini ¹ , Luigi Piarulli ^{1,2}, Marco Miceli ³, Daniela Platano ^{4,5} and Lisa Berti ^{4,5}

- ¹ Movement Analysis Laboratory, IRCCS Istituto Ortopedico Rizzoli, 40136 Bologna, Italy; giulio.sacchetti@ior.it (G.S.); maurizio.ortolani@ior.it (M.O.); leardini@ior.it (A.L.); lp935@drexel.edu (L.P.)
² Department of Mechanical Engineering and Mechanics, Drexel University, Philadelphia, PA 19104, USA
³ Diagnostic and Interventional Radiology Unit, IRCCS Istituto Ortopedico Rizzoli, 40136 Bologna, Italy; marco.miceli@ior.it
⁴ Physical Medicine and Rehabilitation Unit, IRCCS Istituto Ortopedico Rizzoli, 40136 Bologna, Italy; daniela.platano@ior.it (D.P.); lisa.berti@ior.it (L.B.)
⁵ Department of Biomedical and Neuromotor Sciences, University of Bologna, 40127 Bologna, Italy
* Correspondence: belvedere@ior.it

Featured Application: Inclusion of cone-beam computed-tomography scans in weight-bearing, combined with clinical score systems, may lead to more robust pre- and post-operative evaluations of correction surgery following the modified Grice–Green surgical procedure for adult acquired flatfoot, as well as more biomechanically based skeletal investigations of foot alignment.



Citation: Sacchetti, G.; Belvedere, C.; Ortolani, M.; Leardini, A.; Piarulli, L.; Miceli, M.; Platano, D.; Berti, L. Three-Dimensional Bone Alignment from Cone-Beam Computed-Tomography Scans in Weight-Bearing and Clinical Outcomes Following the Modified Grice–Green Surgical Procedure for Adult Acquired Flatfoot. *Appl. Sci.* **2024**, *14*, 8521. <https://doi.org/10.3390/app14188521>

Academic Editor: Miguel Alcaraz

Received: 23 July 2024

Revised: 18 September 2024

Accepted: 19 September 2024

Published: 21 September 2024



Copyright: © 2024 by the authors. Licensee MDPI, Basel, Switzerland. This article is an open access article distributed under the terms and conditions of the Creative Commons Attribution (CC BY) license (<https://creativecommons.org/licenses/by/4.0/>).

Abstract: Severe adult-acquired flatfoot deformity is widely addressed surgically via the Grice–Green subtalar arthrodesis. Standard radiographic measurements have been reported, but these are limited to planar views. These complex deformities and the relevant corrections after surgery should be assessed in weight-bearing using 3D analyses now enabled by modern cone-beam CT scans. The present study is aimed at reporting these 3D radiographical foot bone alignments and the clinical results for this surgery. Ten patients were treated with the Grice–Green procedure. This implies inserting an autologous bone graft from the proximal tibial into the extra-articular sinus-tarsi to perform a subtalar arthrodesis. Before and after surgery, the patients were assessed based on the clinical range-of-motion and Foot-Function and Posture Indexes. Three-dimensional models of the tibia, calcaneus, talus, navicular, and 1st metatarsus were reconstructed from cone-beam CT scans in a single-leg up-right posture. Relevant longitudinal axes were defined to calculate ten spatial angles. Post-operatively, a significant realignment was observed for seven angles, including corrections lift-up of the talus (on average by 15°) and subtalar joint (13° in 3D), as well as the Meary’s angle (21°). Only few correlations were found between traditional clinical and novel 3D radiographical measurements, suggesting the former only limitedly represent the corresponding real skeletal status, and the latter thus offer the physician a more comprehensive evaluation. The present original analysis from modern cone-beam CT scans shows precisely the correction of foot and ankle bone alignments achieved using the Grice–Green surgical procedure, finally in 3D and in weight-bearing. For the first time, traditional clinical and score system evaluations are reported together with bone orientation and joint angles in the three anatomical planes.

Keywords: adult acquired flatfoot; modified Grice–Green surgical procedure; foot clinical outcome; cone-beam computed-tomography; weight-bearing; 3D foot bone alignment

1. Introduction

Adult acquired flatfoot deformity (AAFD) is a symptomatic morphological alteration characterized by the collapse of the medial longitudinal arch (MLA), the abduction of the forefoot, and a valgus rearfoot. This deformity is mainly caused by injury or degeneration of the capsular and ligamentous structures, especially those supporting the foot arches [1], and the long plantar ligament. The main symptom leading to surgery is pain [2], suffered during high-intensity physical activities, such as hiking and running, as well as in less demanding activities, such as standing for a long time. Foot orthoses with forefoot and/or rearfoot posting are conservative options, but with low evidence of significant effects [3]. A number of surgical treatments are available for the most severe cases, combining soft and hard tissues [4–6]: tenodesis of the tibialis posterior tendon; arthrodesis of the collapsed subtalar joint to correct the alignment between the talus and calcaneus [7–9]; lateral column lengthening to restore the arch [10]; calcaneal osteotomy to shift the calcaneus back to a neutral position [10,11].

The goal of these surgeries is to achieve a painless, stable, and functional plantigrade foot. In the case of rigid deformity associated with subtalar osteoarthritis, its arthrodesis is considered the gold standard procedure. Grice–Green subtalar arthrodesis with an autologous bone graft is a widely used surgery [5] given its advantage to correct foot deformities by restoring the physiological alignment among the talus, calcaneus, and navicular bones. A recent study [12] investigated foot alignment via gait analysis using a validated multi-segment foot protocol and showed that the Grice–Green procedure restored frontal-plane alignment of the rearfoot and midfoot, together with a reduction in pain and an improvement in function during daily living activities.

A number of studies have investigated clinical and radiographical outcomes in AAFD patients after surgery, with only a few using modern 3D analyses of foot alignment in weight-bearing derived by cone-beam CT (CBCT) scans [13–15]. This technique can finally provide 3D alignment measurements of the foot bones in a natural weight-bearing condition. There are no studies investigating the effects of the Grice–Green subtalar arthrodesis using CBCT and examining single-bone and joint alignments, finally in 3D and in weight-bearing. Radiographic outcomes before and after subtalar fusion have been reported recently [2,16,17], but these were based on standard bidimensional antero-posterior and lateral views; with these views, a number of bones are obscured, the deformities and corrections in the transverse plane are missed, and calculations of the axial rotation are unfeasible. The Grice–Green seems to be among those surgical procedures particularly likely to obtain benefits from these techniques for the assessment of 3D foot bone alignment. In fact, it is meant to restore this alignment not only on the rear-foot, but also in the mid- and fore-foot, and not only in the sagittal plane, but also in the coronal and transverse anatomical planes.

The aim of this study was to report together and to assess possible correlations between traditional clinical and original 3D radiological outcomes in a population of AAFD patients operated on using the modified Grice–Green procedure.

2. Materials and Methods

2.1. Patient Population

Ten symptomatic stage II AAFD patients (6 females, 4 males; age: 51.3 ± 13.8 years; Body Mass Index (BMI): 28.6 ± 4.2 kg/m²) were recruited in the study. Inclusion criteria were the following: diagnosis of AAFD with an indication for arthrodesis of the subtalar joint via the Grice–Green surgical procedure [8]; age between 18 and 70 years; BMI < 40 kg/m². Exclusion criteria were the following: severe morphological alterations of the foot, foot pathologies other than AAFD, severe neurological and vascular pathologies, and other systemic diseases affecting bone consolidation. The study was approved by the local Ethics Committee (Prot. Gen 0012502, 5 November 2018) and was conducted in accordance with the Declaration of Helsinki. All the participants signed informed consent before participating in the study.

2.2. Surgical Intervention

Patients underwent a modified Grice–Green procedure via arthrodesis of the subtalar joint with an autologous bone graft [7] from the ipsilateral tibia. A 5 cm medial longitudinal incision was performed over the proximal third of the tibia. After passing through the subcutaneous layer, a partial subperiosteal rectangular tibial bone graft was obtained using an oscillating saw. The graft was placed into its bed in the extra-articular sinus tarsi, while forcing the subtalar joint in about 5° valgus. The cancellous bone was used to fill part of the subtalar joint after the placement of the cortical bone graft. After surgery, a non-weight-bearing short leg cast was applied for 40 days to protect both surgical sites, followed by a new weight-bearing cast or walker boot for a further 40 days [2,8].

2.3. Clinical Assessment

Patients' feet were clinically assessed before surgery and at one year of follow-up (9.9 ± 3.5 months) by means of the 17-VAS questions Foot Function Index (FFI) [18] and the Foot Posture Index (FPI) [19,20]. The FFI scale returns a score between 0 and 170, where 0 indicates no pain and no limitation in activities and 170 is associated with the maximum pain and limitations perceived. The FPI scale returns a score between -12 and $+12$, where -12 is associated with a severely supinated foot and $+12$ a severely pronated foot, with 0 representing a normal foot posture. The following passive ranges of motion were measured with a manual goniometer by an experienced operator with the patient lying on a bed: the plantarflexion (TTpla) and the dorsiflexion (TTdorsi) of the tibiotalar joint, i.e., the ankle; the valgus angle of the hallux; the valgus angle of the calcaneus.

2.4. CBCT Scans

Before and after surgery, patients underwent a 3D analysis of foot bone alignments derived from a CBCT scan (OnSight Extremity System, Carestream, Rochester, NY, USA). This provides high-resolution images, with a lower dose of radiation, than conventional CT machines [21]. During image acquisition the patients were asked to stand still upright on the operated leg. This medical imaging technology gives access to the foot anatomy, in 3D and in weight-bearing. The execution time of the exam is 25 s, and a 3D rendering of the foot is returned in a few minutes.

2.5. Three-Dimensional Bone Model Reconstruction

Nine hundred and sixty CT images at a 0.26 mm distance were exported in a Dicom file for each foot scan. This dataset, obtained before and after surgery, was processed in Mimics Innovation Suite version 22.0 (Materialise, Leuven, Belgium) by a single operator to generate a 3D mesh for the distal tibia and fibula and for all the foot bones (Figure 1), i.e., the segmentation process [22]. This entails the separate semi-automatic identification of each bone, starting from the three anatomical views in the Dicom file. The ground under the foot was also segmented and included in the overall 3D model file. This was assumed as the global transverse plane, which was necessary for the calculation of the absolute orientation, i.e., inclination of the foot bones. In the Dicom files of the post-operative CBCT scans, the corticocancellous autograft between the talus and calcaneus (necessarily introduced because of the surgical procedure) was identified and removed; this resulted in a more difficult segmentation of these two bones but did not affect their final 3D pose estimation.

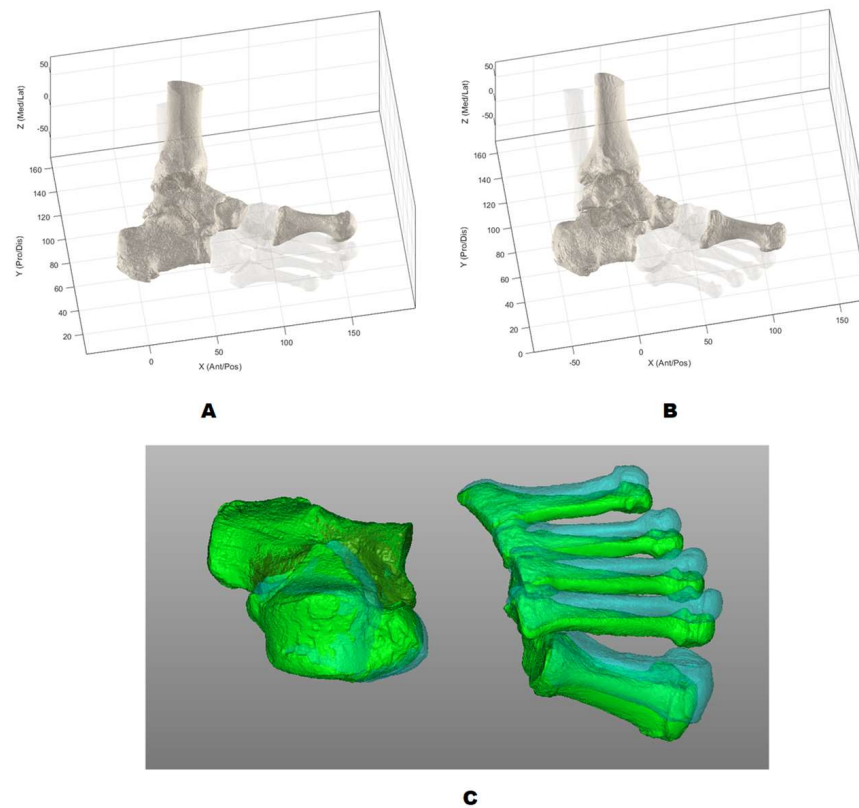


Figure 1. Three-dimensional models of the bones of a left foot (patient #8) before (A) and after (B) surgery, in their anatomical reference frames; with darker grey, those 5 bones here were analyzed for the alignments. The corticocancellous autograft between the talus and calcaneus, definitely scanned after surgery, was removed (B) via the special segmentation procedure performed in the present work. In (C), the two 3D foot models (with mid-foot bones removed) were registered over the calcaneus, for a clearer depiction of all the other changes. The exact corresponding clinical and radiographic measures for this patient can be found in Tables 1 and 2, but the following large corrections can be depicted: CA valgus (both from clinical and radiographic measures), TA and CA orientation in the sagittal plane, TACA and TANA joint angles in the transverse plane. Relevant corrections can also be appreciated at the forefoot (C).

Table 1. Clinical and bone alignment measurements for each patient: pre-operative values.

Pre-Op		Clinical Scores					Bone Alignments									
Patient	FPI	TT Dorsi	TT Pla	Valgism of Allux	Calcaneal Valgism	FFI (%)	IL_TA	IL_CA	I3_CA	RF_TICA	RL_TACA	RT_TACA	R3_TACA	RT_TANA	RL_CAM1	RL_TAM1
#1	12	0	40	5	15	52.4	17.5	-17.2	-17.1	28.1	34.6	-14.0	36.3	-28.7	149.0	-3.6
#2	6	7	45	3	10	67.1	22.6	-12.3	-12.2	41.0	34.9	-21.8	38.9	-42.7	150.3	-5.2
#3	12	10	10	7	15	84.7	27.6	-7.8	-7.8	43.5	35.5	-28.4	41.8	-69.5	161.8	-17.2
#4	12	20	40	15	20	18.2	30.3	-5.3	-5.2	77.9	35.6	-4.7	34.9	-31.2	164.1	-19.7
#5	12	2	25	10	19	67.7	20.5	-7.9	-7.7	61.0	28.3	-4.6	27.9	-53.8	169.2	-17.6
#6	10	20	40	10	20	57.1	34.9	-7.7	-7.5	65.5	42.6	-32.3	46.3	-69.1	159.0	-21.6
#7	12	5	27	4	10	34.7	33.2	-5.0	-5.0	48.9	38.2	-37.0	47.5	-65.0	165.2	-23.3
#8	8	15	45	5	15	79.4	20.9	-11.7	-11.7	39.6	32.7	-12.8	33.8	-39.5	151.9	-4.6
#9	12	0	40	17	10	76.5	21.5	-5.0	-4.9	48.7	26.4	-16.2	29.8	-44.1	162.8	-9.2
#10	10	10	10	5	10	69.4	25.4	-3.1	-3.0	70.1	28.4	-34.6	41.0	-58.5	161.5	-10.0
Mean	10.6	8.9	32.2	8.1	14.4	60.7	25.4	-8.3	-8.2	52.4	33.7	-20.6	37.8	-50.2	159.5	-13.2
SD	2.0	7.5	13.5	4.8	4.2	20.8	5.9	4.3	4.3	15.6	4.9	12.0	6.5	15.1	6.8	7.5

Table 2. Clinical and bone alignment measurements for each patient: post-operative values.

Post-Op		Clinical Scores					Bone Alignments									
Patient	FPI	TT Dorsi	TT Pla	Valgism of Allux	Calcaneal Valgism	FFI (%)	IL_TA	IL_CA	I3_CA	RF_TICA	RL_TACA	RT_TACA	R3_TACA	RT_TANA	RL_CAM1	RL_TAM1
#1	0	2	35	5	15	2.9	6.2	−23.0	−17.7	47.5	29.2	−4.6	23.2	−9.4	133.7	17.1
#2	4	10	45	3	4	12	6.0	−12.2	−11.4	51.6	18.2	−0.7	16.9	−3.4	150.5	11.4
#3	1	10	20	7	15	7.1	15.2	−9.7	−9.7	38.9	25.0	−24.6	34.2	−55.1	156.4	1.5
#4	3	20	35	10	3	5.3	16.7	−10.2	−10.2	43.7	26.9	−5.0	27.3	−1.4	149.7	3.5
#5	5	2	25	6	10	56.5	16.7	−8.0	−7.9	53.3	24.6	−2.6	24.4	−41.1	165.5	10.4
#6	1	20	40	7	6	24.7	15.8	−11.6	−11.3	43.3	27.4	−11.3	29.3	−15.0	150.7	1.9
#7	2	8	30	4	2	25.3	13.2	−7.1	−6.3	56.4	20.3	−17.9	26.2	−20.2	157.4	2.3
#8	3	20	45	5	5	8.2	8.6	−20.7	−19.3	54.0	29.3	−6.2	28.2	−15.1	145.4	5.3
#9	3	5	40	15	4	1.2	3.7	−9.6	−8.8	26.7	13.3	−5.8	13.5	−5.6	156.1	10.6
#10	5	5	25	1	3	8.4	6.2	−5.3	−5.3	47.5	11.5	−22.6	25.0	−32.5	157	11.6
Mean	2.7	10.2	34	6.3	6.7	15.2	10.8	−11.7	−10.8	46.3	22.6	−10.1	24.8	−19.9	152.2	7.5
SD	1.7	7.3	8.8	3.9	4.9	16.7	5.2	5.7	4.5	8.8	6.5	8.6	6.0	17.7	8.6	5.4

2.6. Calculation of Anatomical Planes and Bone Axes

The files with the 3D bone models, in STL format, were imported in Matlab R2021b (Mathworks Inc., Natick, MA, USA) to be processed with original scripts according to an established technique [22]. The first step was the definition of the anatomical reference frame for the entire foot, with the vertical axis orthogonal to the ground plane, the antero/posterior axis on the ground plane joining the projections of the most plantar points of the calcaneus and the second metatarsal head, and the medio/lateral axis orthogonal to these two axes. All bone models were then realigned to this anatomical reference frame.

A reference frame with three anatomical axes was also defined for the tibia (TI), calcaneus (CA), talus (TA), navicular (NA), and 1st metatarsus (M1) according to the standard Principal Component Analysis [22]. Starting from the 3D coordinates of the bone surface points, this statistical analysis implies a one-shot calculation of the three orthogonal axes with the highest variance. For each of these bones, this results in the definition of the longitudinal axis, i.e., the antero-posterior, as well as the medio-lateral and the dorsi-plantar axes. However, for the following angular measurements, only the former was used and projected into the three anatomical planes of the foot, as defined above. Moreover, the plane orthogonal to the ground and passing through the longitudinal axis was defined, to report the most correct inclination, exactly in the spatial plane containing the axis, thus hereinafter called the “3D angle”.

For the assessment of relevant bone alignments before and after the operation, the following ten angles were thus calculated (Figure 2), according to the nomenclature in [22].

IL_TA; IL_CA: the inclination angle in the lateral anatomical plane of the talus (TA) and of the calcaneus (CA), with positive being down to the ground and negative being up.

I3_CA: the inclination angle in 3D of the calcaneus, with negative being up from the ground.

RF_TICA: the relative angle in the frontal anatomical plane between the tibia (TI) and the calcaneus (CA), i.e., varus (negative) and valgus (positive) of the calcaneus.

RL_TACA; RT_TACA; R3_TACA: the relative angle between the talus (TA) and the calcaneus (CA), respectively, in the lateral and transverse anatomical planes, and in 3D.

RT_TANA: the relative angle in the transverse anatomical plane between the talus (TA) and the navicular (NA).

In the transverse anatomical plane, positive values indicate inclinations of the bone toward the lateral side and negative toward the medial side.

RL_CAM1: the relative angle in the lateral anatomical plane between the calcaneus (CA) and the first metatarsal (M1), i.e., the Hibb angle in traditional X-ray pictures [13]; it is the value of the apex dorsi angle.

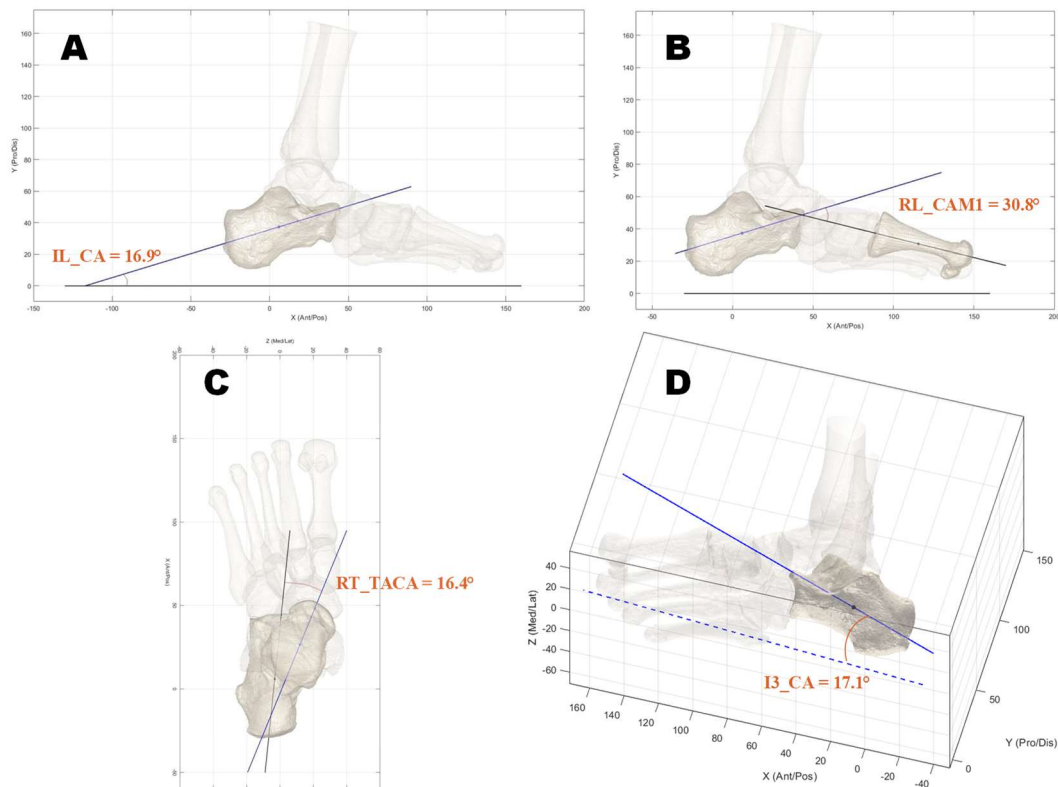


Figure 2. Depiction of four exemplary angles, also with their values (in red), in a typical normal left foot. (A): IL_CA, (B): RL_CAM1, (C): RT_TACA, (D): I3_CA.

RL_TAM1: the relative angle in the lateral anatomical plane between the talus (TA) and the first metatarsal (M1), i.e., the Meary's angle in traditional X-ray pictures [13]; it is the value of the apex dorsii angle and is negative when it is an apex plantar angle.

2.7. Statistical Analysis

The Student *t*-test was used to analyze the statistically significant differences in the measurements, i.e., *p*-values < 0.05, and also incidentally the ability of these techniques to reveal significant differences between pre-op and post-op conditions. Furthermore, the Pearson product-moment coefficient (*R*) was also used to derive possible correlations.

3. Results

3.1. Clinical Assessment

The post-operative clinical condition was found to be improved after surgery (Tables 1 and 2). The high pre-operative values for the FPI and FFI scores, as well as the calcaneal and hallux valgus angles, confirmed the severity of flat foot in all patients. Statistically significant improvements (*p* < 0.001) were found for the FPI (average ± standard deviation: 10.6 ± 2.2 pre-op, 2.7 ± 1.7 post-op), FFI (60.7 ± 20.8% pre-op, 15.2 ± 16.7% post-op), and the calcaneal valgus angle (14.4 ± 4.3 pre-op, and 6.7 ± 4.9 post-op).

3.2. Bone Alignments

Regarding the characterization of bone alignments from CBCT scans (Tables 1 and 2), the severity of the bone orientation and joint deformity of all patients was shown by the pre-operative angles. Post-operatively, a significant improvement was observed for the following 7 out of 10 angles. The drop down of the talus (i.e., IL_TA) was corrected on average by 14.6 ± 5.0° (*R* = −0.81, *p* < 0.001). Significant realignments were also observed at the subtalar joint (i.e., RL_TACA, R3_TACA angles), on average, respectively, 11.2 ± 5.6° (*R* = −0.72, *p* < 0.001) and 13.0 ± 6.6° (*R* = −0.74, *p* < 0.001). Even though not statistically

significant, the calcaneus was elevated in the sagittal plane (i.e., IL_CA) by about 3.5° on average. The MLA, somehow here represented by the RL_CAM1, returned by $7.3 \pm 4.7^\circ$ ($R = -0.44$, $p = 0.05$) to more physiological values. An apex plantar Meary's angle, i.e., RL_TAM1, pre-op ($13.2 \pm 7.5^\circ$) was corrected in an apex dorsal post-op ($7.6 \pm 5.4^\circ$), with an improvement of $20.8 \pm 5.0^\circ$ ($R = 0.86$, $p < 0.001$). Significant realignments were also found in the transverse anatomical plane of the rearfoot, i.e., RT_TANA and RT_TACA. For the former, there was a $30.3 \pm 13.6^\circ$ ($R = 0.70$, $p = 0.001$) reduction in the large extra-rotation of the navicular with respect to the talus; for the latter, there was a $10.5 \pm 7.8^\circ$ ($R = 0.47$, $p = 0.04$) reduction in the large intra-rotation of the talus with respect to the calcaneus. Nevertheless, the degree of correction had a large spectrum of values over the ten patients: from a 13 to even 54° difference in the former and from 0° to 21° in the latter.

Both clinical outcomes and bone alignments showed a large spectrum of values not only over subjects, suggesting that the response to surgery can be different in every case, likely according to age and BMI, but also perhaps according to the severity of the deformity pre-op, the accuracy of the surgery, the laxity of the soft tissues, and the strength of the muscles, etc.

3.3. Correlations between Clinical Assessment and Bone Alignments

Correlations between clinical and angular values were performed both pre- and post-op. Regarding pre-operative data, the only significant correlation was found between the clinical plantarflexion of the tibiotalar joint (TTpla) and the RT_TANA angle ($p = 0.05$, $R = 0.63$), suggesting that the deformity of the talo-navicular joint in the transverse plane is correlated with a reduction in mobility at the ankle. Regarding post-operative data, only four significant correlations were found. A negative correlation ($p = 0.03$, $R = -0.69$) was found between the clinical dorsiflexion of the of the tibiotalar joint (TTdorsi) and the Meary's angle (RL_TAM1). A positive correlation was found between the plantarflexion of the TT joint and both RT_TACA ($p = 0.03$, $R = 0.67$) and RT_TANA ($p = 0.002$, $R = 0.84$) and also between FFI and RF_TICA ($p = 0.0004$, $R = 0.90$). According to these observations, the current traditional clinical assessments of the flat foot, both pre- and post-op, apparently represent only a little of the corresponding real skeletal status.

3.4. Correlations between Pre-Op Condition and the Effects of Corrections

Correlations between pre-op values and the corresponding difference between pre- and post-op were also calculated, both for clinical and alignment measurements. As for the clinical values, statistical significance ($p < 0.01$) was found for FPI and FFI scores and for the TTpla. As expected, all correlations were negative, proving that the most critical clinical cases are those that improved the most. As for the angular values from CBCT, statistical significance ($p = 0.02$) was found for RT_TACA and RL_TAM1, proving that for these two angles, those feet with the largest deformity are those corrected the most.

4. Discussion

The main overall result of this study concerns the technique adopted, from the acquisition of CT scans in upright postures (i.e., using a modern device with the CBCT technology) to the calculation of the bone orientation and joint angles of foot bones. This overall technique was demonstrated to provide, for the first time, thorough alignment measurements of the foot bones in a natural weight-bearing condition. Therefore, the complete skeletal architecture of the flat foot before intervention and the relevant settlement after intervention can be quantified accurately, in 3D and in weight-bearing [13,22], as frequently recommended by physicians [2,8]. This technique overcomes the traditional radiographic measurements, which are less time-consuming and resource-intensive but can provide only bidimensional, mostly only sagittal, measurements of a few basic angles [16,22]. Nevertheless, recent studies in the literature are now also addressing the comparison between traditional and modern radiographic techniques [23]. Accurate 3D bone models were reconstructed using state-of-the-art tools, from which anatomical long axes were defined

via the established Principal Component Analysis [13,22]. Clearly, the latter automatic calculation is independent of manual or other subjective actions or definitions, these being also sometimes affected by the position and orientation of the foot in the radiological device [16,22]. Ultimately these 3D axes show the alignment of the bones in the three anatomical plane projections but also in a spatial view (the so-called 3D angle, Figure 2), exactly in the plane containing the axis, thus overcoming any issue associated with severe deformity or malpositioning of the foot. In fact, this 3D angle was always found to be different from any of its projections in the anatomical planes (Tables 1 and 2).

In particular, this study shows that the modified Grice–Green surgical procedure can improve foot alignment at the talus by correcting its drop down and at the subtalar joint by reestablishing more physiological values of the angle between the talus and the calcaneus in all three anatomical planes (_TACA angles) and also between the talus and the first metatarsal bone (RL_TAM1), i.e., the Meary’s angle. As expected by the surgeons, the 3D corrections observed were not only at the rearfoot where the arthrodesis was performed but also at the forefoot (Figure 1C); this of course cannot be represented by traditional radiography. Possibly because of the improvement in foot alignment, a significant improvement was also observed in the clinical outcomes, with patients showing a larger range of motion of the major foot joints and reporting a better foot function, lower discomfort, and less pain following surgery. In any case, the present encouraging results can now further support the surgeons for the present original surgical technique. The present work also contributes to the recent investigations of possible correlations between radiological and clinical observations, as recommended in the current literature [24]. As mentioned above, a variety of surgical procedures can correct alignment of the foot arches [4–6]. To the best of the authors’ knowledge, the present study is among the few reporting clinical outcomes and bone alignments after surgery in a population with AAFD symptoms, but the same technique can be used for many other corrective surgical treatments on the foot.

In a recent paper, normal values of bony relationships at the normal foot and ankle have been reported in 3D from weight-bearing CT [25]. The study used slightly different techniques for these measures, i.e., bone segmentation and axis calculations, but some of these measurements provide a valuable comparison with the present results. For the calcaneal inclination angle in the sagittal plane (or also calcaneal pitch), i.e., IL_CA, a mean value of 21.9° and a standard deviation of 5.1° were reported; the present trend is from 8.3° pre-op to 11.7° post-op, thus showing for these patients a tendency, however small, toward a more normal inclination of the calcaneus after surgery, which is not obvious knowing the surgical procedure. For the so-called Talar—1st Metatarsal angle in the sagittal plane (Meary’s angle), i.e., RL_TAM1, a mean value of 4.6° (clearly an apex dorsal) and a standard deviation of 6.5° were reported; this compares very well with the present trend from an apex plantar of 13.2° pre-op to the corrected apex dorsal 7.6° post-op, apparently implying a medial longitudinal arch of the present patients that is overcorrected after surgery.

In addition to the present evidence in 3D of a successful correction of the major foot deformities, the present study shows considerable clinical improvements after the modified Grice–Green arthrodesis, according to previous work [2,8,26]. FPI and FFI improved in the present population from preoperative to postoperative, and pain was significantly reduced. The physiologic FPI for a nonpathologically normal arch is approximately +4 [27] or a slightly pronated foot posture, which is consistent with the postoperative FPI observed here. It can be speculated that the pain relief was due to the more physiologic alignment of the middle tarsal joints (calcaneo-cuboid and talo-navicular joints) after subtalar arthrodesis. This may concur with better biomechanics of the foot when walking [12]. Traditional radiographic and score system evaluations can show general improvements after any foot surgery, but these cannot show the exact corrections of the overall foot bone architecture in 3D.

Some limitations should be mentioned for this study. First, this is an initial investigation, which was conducted only on ten patients after the modified Grice–Green method. Additional studies using 3D radiological analyses from CBCT scans but with larger sample

sizes are necessary to further support the present original results. The present measurements focused on the rearfoot, where the surgical correction was performed; the effects on mid- and fore- foot could have been investigated, but this would have been affected by the different stiffnesses of these foot compartments and also would have implied huge datasets. Another issue is the varus/valgus of the calcaneus, i.e., RF_TICA, which is a very difficult measure to take [28], as demonstrated in a previous work by the present authors [29]; nevertheless, in the present work, aimed at comparing pre- versus post-op measurements, the effect of a possible different technique for this angle would be very small. The present thorough 3D analysis implies expensive radiographic devices and software, as well as very time-consuming computer-aided activities of specialized staff (particularly the semi-automatic segmentation). However, the current trend is toward a reduction in the necessary time and relevant costs. Finally, it should be pointed out that due to the emergency situation caused by the COVID19 pandemic, it was not possible to assess the patients at exactly the same follow-ups, with patients evaluated over a large spectrum of times after surgery. Nevertheless, the skeletal architecture achieved at 6 months follow-up in these patients is expected to be maintained afterwards.

5. Conclusions

In conclusion, the present original analysis from modern cone-beam CT scans precisely shows the correction of foot and ankle bone alignments achieved using the Grice–Green surgical procedure, finally in 3D and in weight-bearing. For the first time, traditional clinical and score system evaluations are reported together with bone orientation and joint angles in the three anatomical planes.

Author Contributions: G.S.: Conceptualization, Formal Analysis, Investigation, Methodology, Project Administration, Supervision, Validation, Writing—Original Draft, Writing—Review and Editing. C.B.: Conceptualization, Formal Analysis, Project Administration, Investigation, Methodology, Validation, Writing—Review and Editing, M.O.: Data Curation. Software, Visualization, Formal Analysis, Writing—Review and Editing. A.L.: Conceptualization, Funding Acquisition, Project Administration, Resources, Supervision, Writing—Original Draft, Writing—Review and Editing. L.P.: Data Curation, Formal Analysis, Investigation, Writing—Review and Editing, M.M.: Formal Analysis, Data Curation, Investigation, Resources, Writing—Review and Editing. D.P.: Data Curation, Investigation, Writing—Review and Editing, L.B.: Conceptualization, Project Administration, Resources, Supervision, Investigation, Writing—Review and Editing. All authors have read and agreed to the published version of the manuscript.

Funding: This study was partially funded by the Italian Ministry of Health under the “5 per mille” program.

Institutional Review Board Statement: The study was approved by the ethical committee of the IRCCS Istituto Ortopedico Rizzoli. Bologna—Italy (Prot. Gen 0012502. 5 November 2018). The authors certify that the institution approved the investigation protocol and that all investigations were conducted in compliance with the ethical standards of research.

Informed Consent Statement: Informed consent was obtained from all subjects involved in the study.

Data Availability Statement: Data presented in this study are available upon reasonable request to the corresponding author. The data are not publicly available for privacy reasons.

Conflicts of Interest: There are no conflicts of interest.

References

1. Deland, J.T. The adult acquired flatfoot and spring ligament complex. Pathology and implications for treatment. *Foot Ankle Clin.* **2001**, *6*, 129–135. [[CrossRef](#)] [[PubMed](#)]
2. Mosca, M.; Caravelli, S.; Vocale, E.; Massimi, S.; Fuiano, M.; Grassi, A.; Ceccarelli, F.; Zaffagnini, S. Outcome After Modified Grice-Green Procedure (SAMBB) for Arthritic Acquired Adult Flatfoot. *Foot Ankle Int.* **2020**, *41*, 1404–1410. [[CrossRef](#)] [[PubMed](#)]

3. Desmyttere, G.; Hajizadeh, M.; Bleau, J.; Begon, M. Effect of foot orthosis design on lower limb joint kinematics and kinetics during walking in flexible pes planovalgus: A systematic review and meta-analysis. *Clin. Biomech.* **2018**, *59*, 117–129. [[CrossRef](#)]
4. Haddad, S.L.; Myerson, M.S.; Younger, A.; Anderson, R.B.; Davis, W.H.; Manoli, A., 2nd. Symposium: Adult acquired flatfoot deformity. *Foot Ankle Int.* **2011**, *32*, 95–111. [[CrossRef](#)]
5. Vulcano, E.; Deland, J.T.; Ellis, S.J. Approach and treatment of the adult acquired flatfoot deformity. *Curr. Rev. Musculoskelet. Med.* **2013**, *6*, 294–303. [[CrossRef](#)]
6. Abousayed, M.M.; Alley, M.C.; Shakked, R.; Rosenbaum, A.J. Adult-Acquired Flatfoot Deformity: Etiology, Diagnosis, and Management. *JBJS Rev.* **2017**, *5*, e7. [[CrossRef](#)] [[PubMed](#)]
7. Seymour, N.; Evans, D.K. A modification of the Grice subtalar arthrodesis. *J. Bone Jt. Surg. Br. Vol.* **1968**, *50*, 372–375. [[CrossRef](#)]
8. Mosca, M.; Caravelli, S.; Vannini, F.; Pungetti, C.; Catanese, G.; Massimi, S.; Fuiano, M.; Faldini, C.; Giannini, S. Mini Bone Block Distraction Subtalar Arthrodesis (SAMBB) in the Management of Acquired Adult Flatfoot with Subtalar Arthritis: A Modification to the Grice-Green Procedure. *Joints* **2019**, *7*, 64–70. [[CrossRef](#)]
9. Dennyson, W.G.; Fulford, G.E. Subtalar arthrodesis by cancellous grafts and metallic internal fixation. *J. Bone Jt. Surg. Br. Vol.* **1976**, *58-b*, 507–510. [[CrossRef](#)]
10. Trnka, H.J.; Easley, M.E.; Myerson, M.S. The role of calcaneal osteotomies for correction of adult flatfoot. *Clin. Orthop. Relat. Res.* **1999**, *365*, 50–64. [[CrossRef](#)]
11. Colo, G.; Mazzola, M.A.; Pilone, G.; Dagnino, G.; Felli, L. Lateral open wedge calcaneus osteotomy with bony allograft augmentation in adult acquired flatfoot deformity. *Clin. Radiol. Results. Eur. J. Orthop. Surg. Traumatol. Orthop. Traumatol.* **2021**, *31*, 1395–1402. [[CrossRef](#)] [[PubMed](#)]
12. Caravaggi, P.; Rogati, G.; Leardini, A.; Bevoni, R.; Girolami, M.; Berti, L. Clinical and multi-segment kinematic analysis of a modified Grice arthrodesis to correct type II adult-acquired flat-foot. *Gait Posture* **2023**, *100*, 268–275. [[CrossRef](#)] [[PubMed](#)]
13. Ortolani, M.; Leardini, A.; Pavani, C.; Scicolone, S.; Girolami, M.; Bevoni, R.; Lullini, G.; Durante, S.; Berti, L.; Belvedere, C. Angular and linear measurements of adult flexible flatfoot via weight-bearing CT scans and 3D bone reconstruction tools. *Sci. Rep.* **2021**, *11*, 16139. [[CrossRef](#)]
14. Day, J.; de Cesar Netto, C.; Nishikawa, D.R.; Garfinkel, J.; Roney, A.; O'Malley, J.M.; Deland, T.J.; Ellis, J.S. Three-Dimensional Biometric Weightbearing CT Evaluation of the Operative Treatment of Adult-Acquired Flatfoot Deformity. *Foot Ankle Int.* **2020**, *41*, 930–936. [[CrossRef](#)]
15. de Cesar Netto, C.; Barbachan Mansur, N.S.; Lalevee, M.; Carvalho, K.A.M.; Godoy-Santos, A.L.; Kim, K.C.; Lintz, F.; Dibbern, K. Effect of Peritalar Subluxation Correction for Progressive Collapsing Foot Deformity on Patient-Reported Outcomes. *Foot Ankle Int.* **2023**, *44*, 1128–1141. [[CrossRef](#)] [[PubMed](#)]
16. Vacketta, V.G.; Jones, J.M.; Catanzariti, A.R. Radiographic Analysis and Clinical Efficacy of Hindfoot Arthrodesis with Versus Without Cotton Osteotomy in Stage III Adult Acquired Flatfoot Deformity. *J. Foot Ankle Surg. Off. Publ. Am. Coll. Foot Ankle Surg.* **2022**, *61*, 879–885. [[CrossRef](#)]
17. Conti, M.S.; Garfinkel, J.H.; Ellis, S.J. Outcomes of Reconstruction of the Flexible Adult-acquired Flatfoot Deformity. *Orthop. Clin. North. Am.* **2020**, *51*, 109–120. [[CrossRef](#)]
18. Budiman-Mak, E.; Conrad, K.J.; Roach, K.E. The Foot Function Index: A measure of foot pain and disability. *J. Clin. Epidemiol.* **1991**, *44*, 561–570. [[CrossRef](#)]
19. Redmond, A.C.; Crosbie, J.; Ouvrier, R.A. Development and validation of a novel rating system for scoring standing foot posture: The Foot Posture Index. *Clin. Biomech.* **2006**, *21*, 89–98. [[CrossRef](#)]
20. Martinelli, N.; Scotto, G.M.; Sartorelli, E.; Bonifacini, C.; Bianchi, A.; Malerba, F. Reliability, validity and responsiveness of the Italian version of the Foot Function Index in patients with foot and ankle diseases. *Qual. Life Res. Int. J. Qual. Life Asp. Treat. Care Rehabil.* **2014**, *23*, 277–284. [[CrossRef](#)]
21. Ludlow, J.; Ivanovic, M. Weightbearing CBCT, MDCT, and 2D imaging dosimetry of the foot and ankle. *Int. J. Diagn. Imaging* **2014**, *1*, 9. [[CrossRef](#)]
22. Carrara, C.; Belvedere, C.; Caravaggi, P.; Durante, S.; Leardini, A. Techniques for 3D foot bone orientation angles in weight-bearing from cone-beam computed tomography. *Foot Ankle Surg. Off. J. Eur. Soc. Foot Ankle Surg.* **2021**, *27*, 168–174. [[CrossRef](#)] [[PubMed](#)]
23. Richter, M.; Lintz, F.; de Cesar Netto, C.; Barg, A.; Bursens, A. Results of more than 11,000 scans with weightbearing CT—Impact on costs, radiation exposure, and procedure time. *Foot Ankle Surg.* **2020**, *26*, 518–522. [[CrossRef](#)]
24. Poutoglidou, F.; Marsland, D.; Elliot, R. Does foot shape really matter? Correlation of patient reported outcomes with radiographic assessment in progressive collapsing foot deformity reconstruction: A systematic review. *Foot Ankle Surg.* **2024**, *30*, 441–449. [[CrossRef](#)]
25. Zaidi, R.; Sangoi, D.; Cullen, N.; Patel, S.; Welck, M.; Malhotra, K. Semi-automated 3-dimensional analysis of the normal foot and ankle using weight bearing CT - A report of normal values and bony relationships. *Foot Ankle Surg.* **2023**, *29*, 111–117. [[CrossRef](#)]
26. Kitaoka, H.B.; Alexander, I.J.; Adelaar, R.S.; Nunley, J.A.; Myerson, M.S.; Sanders, M. Clinical rating systems for the ankle-hindfoot, midfoot, hallux, and lesser toes. *Foot Ankle Int.* **1994**, *15*, 349–353. [[CrossRef](#)]
27. Redmond, A.C.; Crane, Y.Z.; Menz, H.B. Normative values for the Foot Posture Index. *J. Foot Ankle Res.* **2008**, *1*, 6. [[CrossRef](#)] [[PubMed](#)]

28. Williamson, E.R.; Chan, J.Y.; Burket, J.C.; Deland, J.T.; Ellis, S.J. New radiographic parameter assessing hindfoot alignment in stage II adult-acquired flatfoot deformity. *Foot Ankle Int.* **2015**, *36*, 417–423. [[CrossRef](#)]
29. Pavani, C.; Belvedere, C.; Ortolani, M.; Girolami, M.; Durante, S.; Berti, L.; Leardini, A. 3D measurement techniques for the hindfoot alignment angle from weight-bearing CT in a clinical population. *Sci. Rep.* **2022**, *12*, 16900. [[CrossRef](#)]

Disclaimer/Publisher’s Note: The statements, opinions and data contained in all publications are solely those of the individual author(s) and contributor(s) and not of MDPI and/or the editor(s). MDPI and/or the editor(s) disclaim responsibility for any injury to people or property resulting from any ideas, methods, instructions or products referred to in the content.